Supporting Information

Figure S1 : Cyclic voltammetry of $[Mo_2(cp)_2(\mu\text{-}SMe)_3(\mu\text{-}\eta^1\text{-}N_2HPh)]^+$, **1-H$^+$** (ca 0.8 mM) in thf-$[NBu_4][PF_6]$ (vitreous carbon electrode, v = 0.2 V s^{-1}).

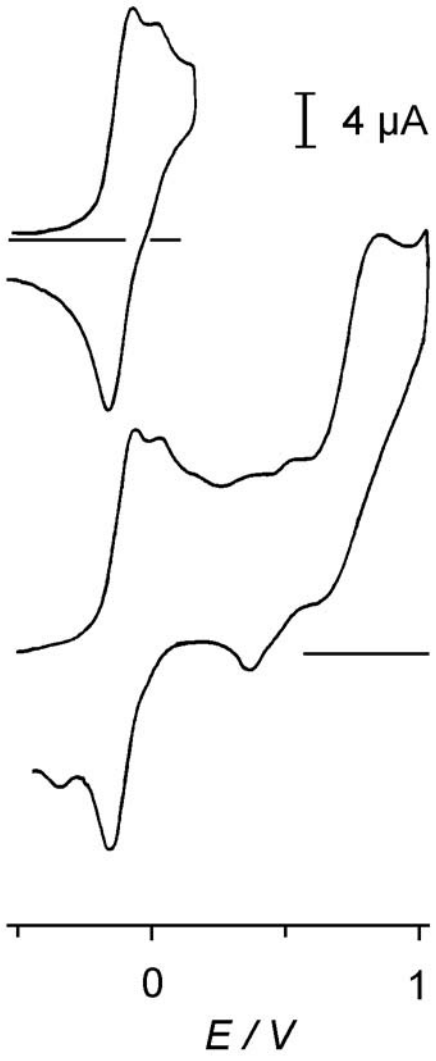

Figure S2 : Cyclic voltammetry of $[Mo_2(cp)_2(\mu\text{-}SMe)_3(\mu\text{-}\eta^1\text{:}\eta^1\text{-}HN_2Ph)]^+$, (present essentially as **2-H$^+$**) formed in situ from **1-H$^+$** (ca 0.8 mM) (see figure S1) in thf-$[NBu_4][PF_6]$ (vitreous carbon electrode, v = 0.2 V s^{-1}).

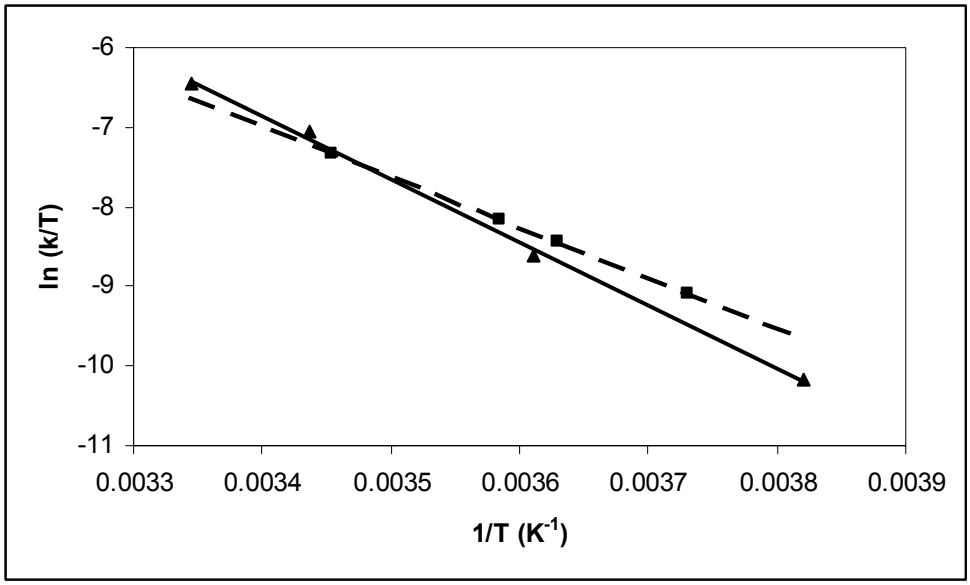

Figure S3 : Eyring plots of kinetic data for the μ-η^1 → μ-η^1:η^1 isomerization of [$Mo_2(cp)_2$(μ-$SMe)_3$(μ-N_2Ph)] in thf (▲) and in CH_2Cl_2 (■); the lines represent the least-square plots in thf (—; R^2 = 0.998) and in CH_2Cl_2 (- - -; R^2 = 0.999).

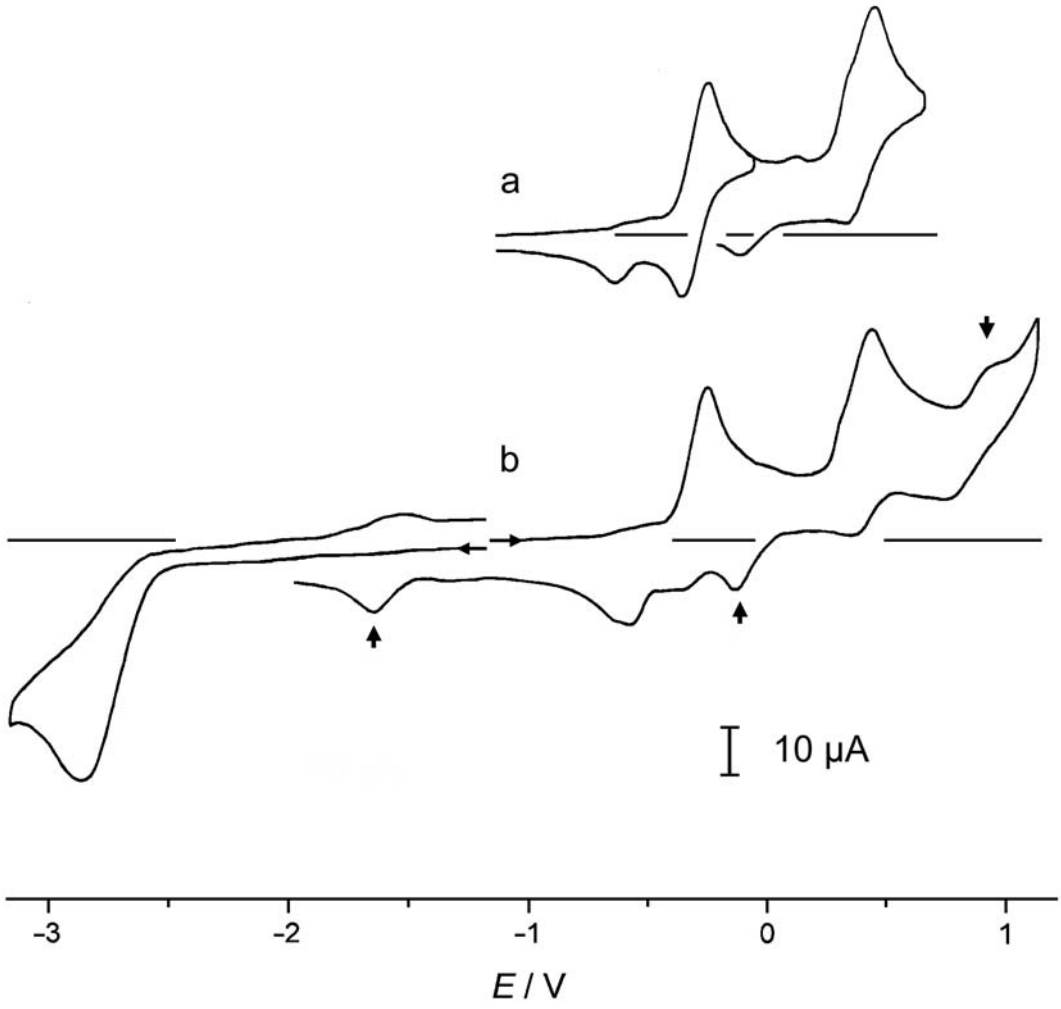

Figure S4 : Cyclic voltammetry of $[Mo_2(cp)_2(\mu\text{-}SMe)_3(\mu\text{-}\eta^1\text{-}N_2Ph)]$, **1** (1.2 mM) in thf–$[NBu_4][PF_6]$. Curve b) shows the characteristic redox processes of the diazene complex **2-H^{2+}** (arrows); that the reduction peak around –1.6 V arises from oxidation of **1** is shown by its absence in the negative-going scan (T = 18°C; vitreous carbon electrode; v = 0.2 V s^{-1}).

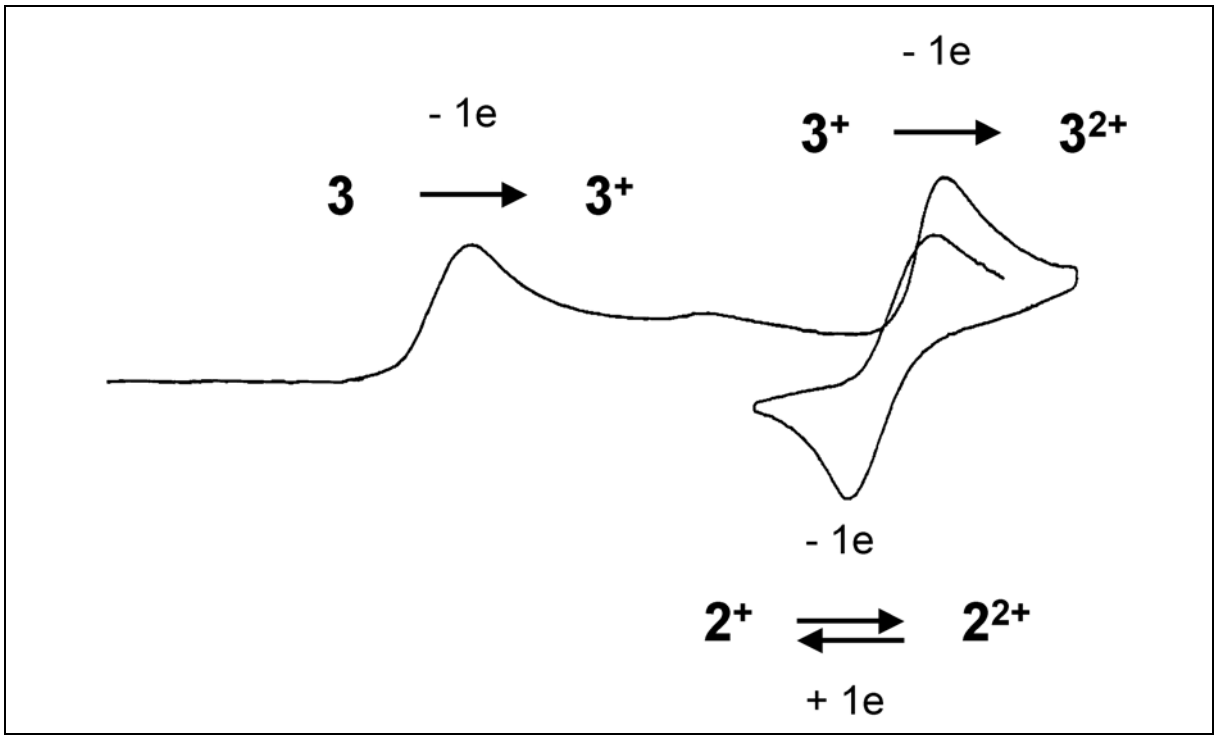

Figure S5 : Cyclic voltammetry of *syn*-[$Mo_2(cp)_2(\mu\text{-}SMe)_3(\mu\text{-}\eta^1\text{:}\eta^1\text{-}N_2Ph)$], **3** in CH_2Cl_2-$[NBu_4][PF_6]$ at –46°C showing the reversible (*anti*) $\mathbf{2^{2+}/2^{+}}$ couple at a potential slightly less positive than the onset of the oxidation of $\mathbf{3^{+}}$ (v = 0.1 V s^{-1}; vitreous carbon electrode).